ISSN 1027-5495. Functional Materials, 27, No.2 (2020), p. 252-257.
doi:https://doi.org/10.15407/fm27.02.252

Photopolarization of undoped and gallium doped crystals of silicosillenites

T.V.Panchenko[1], *L.M.Karpova*[2]

[1]O. Honchar Dnipro National University, 72 Gagarin Ave., 49010 Dnipro, Ukraine
[2]Ukrainian State University of Chemical Technology, 8 Gagarin Ave., 49005 Dnipro, Ukraine

Received November 13, 2019

The effect of visible light on polarization processes in undoped and gallium doped crystals of silicosillenites ($Bi_{12}SiO_{20}$ and $Bi_{12}SiO_{20}$:Ga) was studied using thermoactivation, photo- and dielectric spectroscopy in the temperature range of 300 to 800 K. The temperature dependences of the current of thermally stimulated depolarization and dielectric permitivity, polarization charge, and dielectric hysteresis loops under different polarization conditions are obtained, and the mechanisms of space-charge and quasi-dipole polarization are identified.

Keywords: photopolarization, thermally stimulated depolarization, dielectric permitivity, undoped and gallium doped crystals of silicosillenites.

Методами термоактивационной, фото- и диэлектрической спектроскопии в области температур 300–800 К исследовано влияние света видимого диапазона на поляризационные процессы в нелегированных и легированных галлием кристаллах силикосилленитов ($Bi_{12}SiO_{20}$ и $Bi_{12}SiO_{20}$:Ga, соответственно). Получены температурные зависимости тока термостимулированной деполяризации и диэлектрической проницаемости, поляризационного заряда и петель диэлектрического гистерезиса при различных условиях поляризации, идентифицированы механизмы объемно-зарядовой и квазидипольной поляризации.

Фотополяризація нелегованих і легованих галієм кристалів силікосиленітів. *Т.В.Панченко, Л.М.Карпова.*

Методами термоактиваційної, фото- та діелектричної спектроскопії в області температур 300–800 К досліджено вплив світла видимого діапазону на поляризаційні процеси у нелегованих та легованих галієм кристалах силікосиленітів ($Bi_{12}SiO_{20}$ та $Bi_{12}SiO_{20}$:Ga, відповідно). Отримано температурні залежності струму термостимульованої деполяризації і діелектричної проникності, поляризаційного заряду і петель діелектричного гістерезису за різних умов поляризації, ідентифіковано механізми об'ємно-зарядової та квазідипольної поляризації.

1. Introduction

Photorefractive crystals of sillenites $Bi_{12}MO_{20}$ (BMO, where M = Si, Ge, and Ti) which possess a unique combination of many practically useful properties are comprehensively studied. In recent decades, $Bi_{12}SiO_{20}$ (BSO), $Bi_{12}GeO_{20}$ (BGO) and $Bi_{12}TiO_{20}$ (BTO) crystals have been used as an active medium in devices for recording and processing optical information in real-time, holographic interferometry, and optoelectronic devices of different types [1, 2]. At the same time, the range of practical application of BMO is constantly expanded. For example, it has been proposed to use BSO and BGO as fiber-optic sensors for the study of magnetic fields and electric currents [3].

For practical purposes, it is necessary to optimize the conditions of functioning and technical characteristics of BMO, which are largely determined by the photoelectric

processes. It is important to modify the properties of sillenites and to improve their functional parameters by doping. The character of influence of many impurity ions (Al, Ga, Cr, Mn, Cu, Mo and some others) on the photochromic effect (PCE), optical absorption and photoconductivity of BMO is known. In particular, the Al and Ga ions cause a decrease in the optical absorption edge, photoconductivity and PCE, while Cr and Mn ions are responsible for enhancement of these characteristics [4–6]. In addition, at present, the attention of researchers is focused on the role of phenomena and processes that accompany the photorefractive and electro-optical effects. It has been established that under certain conditions, the optical activity, PCE, piezoelectric effect, photovoltaic and flexoelectric effects must be taken into account [7–11].

In this regard, insufficient attention has been paid to the processes of polarization in BMO crystals. Thermal depolarization analysis of dark polarization of BSO crystals undoped and doped with Al, Ga, Cr and Mn ions was performed [12, 13], while the effect of light on polarization features and dielectric properties of undoped and doped BMO was not considered in detail. However, such processes can influence on the dynamics of the photorefractive response of sillenites [14], the nonlinear interaction of moving gratings of space charge and photoconductivity, the formation of a photo-induced space charge and the motion of waves of spatial re-charge of traps in the forbidden gap [15]; therefore attention to the photopolarization of BMO is sufficiently justified.

In this work, the photostimulated polarization, depolarization, and dielectric properties of BSO and $Bi_{12}SiO_{20}$:Ga (BSO:Ga) crystals were experimentally investigated. The choice of Ga ions as a dopant was due to their significant influence on the photoelectric properties and thermally stimulated polarization of BMO crystals [6, 13].

2. Experimental

Optically homogeneous crystals of BSO and BSO:Ga were grown by the Czochralski method. The content of Ga in BSO:Ga crystals was 0.02 mass % according to spectral-emission analysis. Samples were prepared in the form of polished bars in sizes of (1–1.5)×3×5 mm^3 with a surface area of (1–1.5)×5 mm^2 cut in the crystallographic plane (001). Platinum electrodes were deposited on a surface measuring 3×5 mm^2 by cathodic sputtering in vacuum. Since the dark resistivity of BSO is high ($\rho \sim 10^{14}$ Om·cm), the samples were placed in a crystalline holder with sapphire insulation ($\rho \sim 10^{19}$ Om·cm). The samples were heated to 900 K before measurements, and after slow cooling during the day, they were illuminated with red light ($\lambda = 0.63$ μm). This procedure ensured reproducibility of the results.

Photopolarization of the samples was carried out under conditions of a constant electric field; the field strength and polarization temperature were $E_p = 1 \div 5$ kV·cm^{-1} and $T_p =$ 250 K, respectively; the energy of the light quanta for photo-activation of the polarization, $h\nu_p$, changed from 1.3 to 3.5 eV. The duration of polarization was 30 minutes in all cases. During photopolarization, the light was directed perpendicularly to the action of the electric field **E**. This excluded an inhomogeneous distribution of the concentration of photoexcited charge carriers along **E**.

The currents of thermally stimulated polarization and depolarization (TSD) were measured in a temperature range of 300–800 K in the linear heating mode with a speed of $\beta = 0.16$ K·s^{-1}. The measurements were automated using a micro-computer.

The effect of photopolarization on the dielectric properties was analyzed by the temperature dependences of the real part of the complex dielectric permittivity $\varepsilon'(T)$ at a frequency of 100 Hz before and after polarization under the same conditions that were used to register the TSD currents. A P5085 AC bridge provided an automatic selection of the nature of the reactivity of the equivalent circuit of the test samples. In addition, the voltage-farad characteristics (VFCs) were measured, namely, the dependences of the capacitance on the value of the applied DC bias voltage $C(U_b)$. During the measurements, the voltage U_b varied discretely with a step of ±5 V and a pause of ~ 30 s; its duration was much longer than the Maxwell relaxation time for sillenites (~ 0.1 s). The voltage changed cyclically with variations of sign: $0 \rightarrow +200$ V $\rightarrow 0 \rightarrow -$ 200 V $\rightarrow 0$; the E8-4 bridge was used.

Stationary and photo-induced photoconductivity were measured at room temperature on the samples of crystals prepared in the form of polished plates. Silver electrodes were deposited on the crystallographic surfaces (001) of the plates; the gap between the electrodes was 0.7÷1.0 mm. An SDM-2 monochromator with a resolution of ~ 0.02 eV was used. The spectral dependences of the photoconductivity $\Delta\sigma^{ph}(h\nu)$ were normalized with

Table. Polarization charge and characteristics of electrically active defects of BSO and BSO:Ga crystals

	Dark polarization				Photopolarization				
Function Parameter/Crystal	$Q_p \cdot 10^6$, C	$I^{TSD}(T)T_{max}$, K	E_a, eV	$\varepsilon'(T)$ T_{max}, K	$Q_p \cdot 10^6$, C	$I^{TSD}(T)T_{max}$, K	E_a, eV	$h\nu_p$, eV	$\varepsilon'(T)$ T_{max}, K
BSO	2.8	693	0.81	642	9.3	595	0.79	1.86	735
				738	2.19	579	0.48	2.79	
				752	7.13	619	0.84	2.86	665
									735
					16.94	530	0.76	3.08	
						480	0.71		
BSO:Ga	30.8	361	0.61	595	22.9	361	0.61	1.86	623
						390	0.64		754
						503	0.83		
		390	0.64	643	24.4	361	0.61	2.79	
						393	0.64		
						503	0.83		
		503	0.83	741	37.5	361	0.61	2.86	557
						399	0.66		623
						503	0.83		
					43.1	361	0.61	3.08	
						402	0.66		
						503	0.83		

respect to the apparatus function of the spectral distribution of the photon flux.

The temperature dependences of the TSD currents, i.e. the $I^{TSD}(T)$ spectra, and dielectric permittivity, $\varepsilon'(T)$, were obtained before and after the "dark" polarization of the samples without photo-stimulating light; the results indicate a significant effect of Ga ions on the electrophysical properties of BSO (Fig. 1a, b).

2. Results and discussion

Ga ions cause a significant low-temperature shift of the $I^{TSD}(T)$ spectrum, an increase in the intensity and a change in the shape of its main peak from a structured dome shape for BSO (T_{max} = 693 K) to a narrow almost symmetrical shape for BSO:Ga (T_{max} = 503 K); also, additional low-temperature peaks at T_{max} = 361 and 390 K appear. Such a metamorphosis of the spectra indicates a participation of electrically active defects with different energies of the thermal activation E_a and also a different accumulated polarization charge Q_p in the polarization. The presence of low-temperature slopes in several peaks make it possible to use the

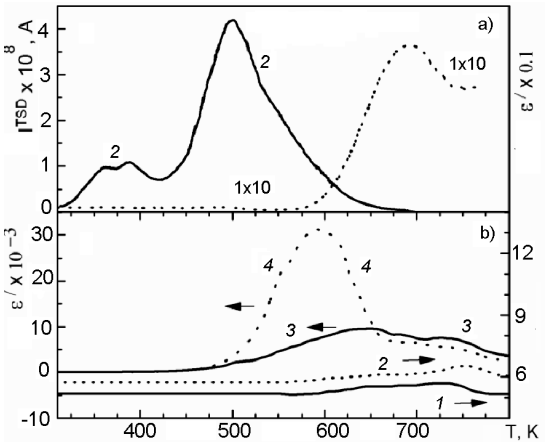

Fig. 1. Spectra of TSD current (a) of BSO (a, 1) and BSO:Ga (a, 2) crystals after polarization in the dark and temperature dependences of dielectric permittivity (b) of BSO crystals (b, 1, 2) and BSO:Ga (b, 3, 4) before (b, 1, 3) and after (b, 2, 4) dark polarization.

initial slope method and find the value of $E_a = d(\ln(I(T))/d(1/kT)$, where k is the Boltzmann constant. Further, considering that the obtained values satisfy the relation $E_a = AkT_{max}$, the value of A was determined [16]. This made it possible

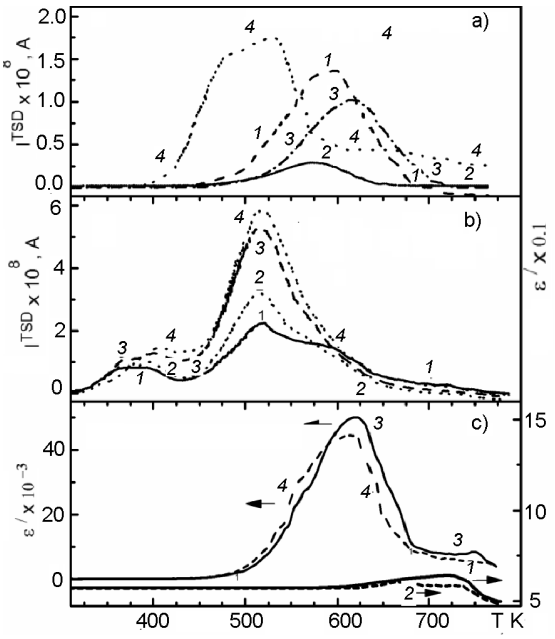

Fig. 2. Spectra of TSD current of BSO (a) and BSO:Ga (b) crystals after photopolarization with $h\nu_p$ = 1.86 (a, 1, b, 1), 2.79 (a, 2, b, 2), 2.86 (a, 3, b, 3) and 3.08 eV (a, 4, b, 4); temperature dependences of the dielectric permitivity (c) of BSO (c, 1, 2) and BSO:Ga (c, 3, 4) crystals after photopolarization with $h\nu_p$ = 1.86 (c, 1, 3) and 2.86 eV (c, 2, 4).

to find the values of E_a for the remaining peaks from the temperature position of the maxima under the assumption that A depends only on the type of crystal. The advantage of the used methods is that the obtained E_a do not depend on the kinetics of relaxation processes and on the polarization mechanisms (space-charge or quasi-dipole ones). The polarization charge was determined as $Q_p = \int_0^t I(t)dt$ with using the dependence $T = T_0 + \beta t$, where T_0 = 300 K, t is time (Table 1).

In the initial state (before polarization) the $\varepsilon'(T)$ dependences of the BSO:Ga crystals, like the $I^{TSD}(T)$ spectra, are somewhat shifted to the low-temperature region relative to those for BSO crystals. After polarization, the shift of the $\varepsilon'(T)$ curves for the BSO:Ga crystals increases, so that they fall in the same temperature range as the $I^{TSD}(T)$ spectra, whereas low-temperature peaks are not registered. The charge Q_p is significantly higher than for undoped crystals (Table). After polarization of the BSO crystals, a weak high-temperature shift of $\varepsilon'(T)$ is observed (Fig. 1a, b).

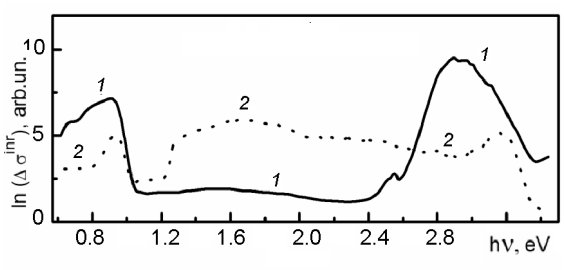

Fig. 3. Spectra of the photoconductivity of BSO (*1*) and BSO:Ga (*2*) crystals induced by ultraviolet light.

The photopolarization of the BSO crystals significantly changes the general appearance of the peaks of the $I^{TSD}(T)$ spectra; their temperature positions shift to the low-temperature region (Fig. 1a, 2a). In this case, new peaks are registered and the value of the photopolarization charge Q_p increases for light with energies $h\nu_p$ = 1.86, 2.86, and 3.08 eV and decreases for light with $h\nu_p$ = 2.79 eV relative to the Q_p values of the dark polarization (Fig. 2a, Table). The $\varepsilon'(T)$ dependences react weakly to photopolarization (Fig. 2c, 1, 2).

In contrast to BSO, the photopolarization of the BSO:Ga crystals weakly changes the general appearance of the $I^{TSD}(T)$ spectra. However, a high-temperature shift of the peak at T_{max} = 390 K is observed, following an increase in energy of quantum $h\nu_p$. The temperature positions of the remaining peaks do not change (Fig. 2b). The polarization charge grows (but insignificantly) with increasing energy of quantum $h\nu_p$ (Fig. 2b, Table). The $\varepsilon'(T)$ dependences respond to photo-polarization similarly to the $I^{TSD}(T)$ spectra (Fig. 2c).

Different effects of photoactivation on the polarization of the BSO and BSO:Ga crystals might be caused by a different ratio between the contributions of the space-charge and quasidipole polarization. The low-temperature shift of the TSD current peaks and the change in the charge Q_p after the photopolarization of BSO crystals indicate the space-charge polarization mechanism and the bimolecular kinetics of Q_p relaxation with a strong re-capture of charge carriers in the traps of the forbidden gap. In this case, the value of Q_p increases, and T_{max} decreases with an increase in the degree of initial filling of the traps by electrons [16]. Photoexcitation with different energies $h\nu_p$ favors filling the traps to different degrees.The spectral dependences $Q_p(h\nu_p)$ corre-

late with the dependences of the photo-induced photoconductivity $\Delta\sigma^{inr}(h\nu)$, where $\Delta\sigma^{inr} = \Delta\sigma^{in}/\Delta\sigma^{st}$, $\Delta\sigma^{in}$ is the additional photoconductivity induced by ultraviolet light, and $\Delta\sigma^{st}$ is the initial photoconductivity. In other words, the highest values of Q_p fall on the spectral regions $h\nu_1 = 0.8–1$ eV and $h\nu_2 = 2.5–3.5$ eV of the maximum increase of $\Delta\sigma^{inr}$ (Fig. 3 and 1, Table). The thermal activation energy of the peaks of the $I^{TSD}(T)$ spectra lies in the range $E_a = 0.48–0.84$ eV (Table); that indicates the participation of several types of traps in the charge accumulation.

In the case of BSO:Ga, the high-temperature shift of the peak with $T_{max} = 390$ K indicates the contribution of the space-charge polarization for the case of the quasi-continuous energy distribution of shallow traps and the strong re-capture of charge carriers in them. The dominant mechanism that causes the appearance of an intense non-shifted peak of the TSD current at $T_{max} = 503$ K might be either the quasi-dipole or space-charge polarization with monomolecular kinetics of relaxation and weak re-capture of charge carriers into traps [16]. Taking into account the results of the analysis of dark thermodepolarization currents [13] and the large value of the polarization charge Q_p which makes it possible to exclude a weak re-capture of electrons into traps, the quasidipole mechanism can be considered the most probable. Some correlation between the spectral dependences $Q_p(h\nu_p)$ and $\Delta\sigma^{inr}(h\nu)$ is unusual (Fig. 3 and 2, Table), since the Ga impurity reduces the BSO photoconductivity by 3–4 orders of magnitude in the entire studied spectral range [6].

It is noteworthy that in both cases, the dark polarization and especially the photopolarization entails an increase in the numerical values of ε' obtained in the high-temperature region up to $\varepsilon' \sim 10^4$ for BSO:Ga and $\varepsilon' \sim 10^2$ for BSO (Fig. 2c). However, we note that the values $\varepsilon' \sim 10^4–10^5$ at $300 < T < 500$ K were already observed at measurement frequencies from 1 to 10^3 Hz for undoped and cobalt doped BGO crystals, similar in structure and close in properties to BSO [17]. The authors of [17] attribute the high values of ε' and the features of dielectric relaxation to the incorporation of cobalt in the form of metallic nanoparticles into the dielectric BGO matrix. This seems unlikely, since the ions of the metal usually react with the matrix and form oxide inclusions.

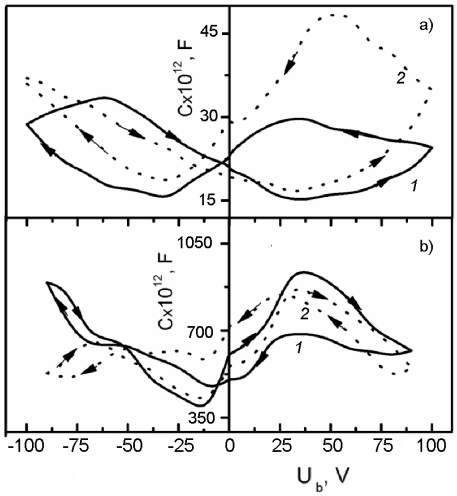

Fig. 4. Voltage-farad characteristics of BSO (a) and BSO:Ga (b) crystals after photopolarization with $h\nu_p = 1.86$ (a, 1, b, 1) and 2.86 eV (a, 2, b, 2).

An interesting evidence of the dielectric nonlinearity of the investigated crystals is demonstrated by the VFCs (Fig. 4). In both cases of BSO and BSO:Ga, they are not linear and have the form of hysteresis loops. The hysteresis area in the first measurement cycle is much larger than in the second, and does not change in subsequent cycles. It depends on the energy of the photoactivation quanta $h\nu_p$ and is maximum after photopolarization by the blue light ($h\nu_p = 2.86$ eV) for BSO and by the red light ($h\nu_p = 1.86$ eV) for BSO:Ga. For BSO, the hysteresis is conditionally "positive", i.e. the forward capacitance is less than the reverse measurement capacitance, while for BSO:Ga it is vice versa "negative". The influence of the Ga dopant leads to a significant increase in the dielectric permitivity (ceteris paribus) and in the deformation of the hysteresis loops $C(U_b)$ (Fig. 4).

For the analysis of the VFCs, it is necessary to take into account the conditions of photopolarization and the formation of a photoelectret state (FES). The fact that the work function of electrons from BSO is $F_1 = 4.5$ eV [18], and from platinum $F_2 = 5.6$ eV indicates the type of Pt–BSO contacts, similar to the Schottky barriers, which excludes the injection of electrons from Pt. In the absence of photoactivation, the hysteresis loops of the $C(U_b)$ curves are symmetrical similar to the "butterfly" wings. The formation of a FES with $h\nu_p = 2.86$ eV violates this symmetry, since the photoinduced charge is accumulated near one of the

electrodes (Fig. 4). The obtained shape of the $C(U_b)$ curves indicates a reorientation of the internal field of the electret under the action of bias voltage, similar to the reorientation of domains in ferroelectrics.

Further, it is necessary to take into account the similarity of the optical and dielectric properties of BTO and $Bi_4Ti_3O_{12}$ from the families of sillenites and perovskites, respectively, as was noted in [19]. Proceeding from the isostructurality BTO and BSO crystals [20], we also rely on the results of studies of the VFCs and dielectric hysteresis in perovskite crystals of $SrTiO_3$ [21]. The hysteresis state in the form of dome-shaped $C(U_p)$ dependences was attributed by the authors of [21] to the formation of a space charge in the near-electrode regions, which is due to the capture of electrons in the forbidden-gap traps. While, a positive hysteresis confirms the absence of injection (Fig. 4a). Doping with Ga leads to a sharp increase in the dark electroconductivity of BSO:Ga crystals, therefore, the ratio between F1 and F2 can change so that the injection of electrons becomes possible. As a result, a monoelectret state is formed. The internal field of the monoelectret causes distortion of the hysteresis loops, while the hysteresis is negative (Fig. 4b). However, the sharp increase in the dielectric permittivity, the anomalous temperature dependences $\varepsilon'(T)$ and the dielectric non-linearity of the hysteresis loops caused by Ga ions can difficultly be explained only by accumulation of the near-electrode space charge .

These features of the dielectric properties of BSO:Ga crystals are similar to those of Aurivillius (FA) phases containing Bi and Ga. FAs are a family of layered perovskite-like Bi compounds. In particular, in $Bi_5Ca_{0.5}GaTi_{3.5}O_{16.5}$ crystals, an increase in ε' caused by Ga was also observed, as well as high-temperature peaks of the $\varepsilon'(T)$ dependences and hysteresis loops. The latter are attributed to the ferroelectric properties of crystals [22]. The nature of the $\varepsilon'(T)$ peaks, hysteresis loops, and the role of Ga in BSO:Ga crystals requires additional studies.

4. Conclusions

It was found that the Ga doping in BSO:Ga crystals causes a significant increase in the dielectric permittivity constant and the appearance of anomalous dependences $\varepsilon'(T)$ in the region $T > 500$ K; these correlate with the temperature dependences of the current of thermally stimulated depolarization. It was shown that the photopolarization by visible light and varying the conditions of polarization in the dark makes it possible to effectively control the high-temperature features of $\varepsilon'(T)$ and the evolution of the dielectric hysteresis loops of BSO:Ga crystals.

This work was supported by the Ministry of Education and Science of Ukraine (theme No. 6-647-19).

References

1. P.Gunter, J.Huignard, Photorefractive Materials and Their Applications, Part 1. Springer Science+Business Media, New York (2006).
2. P.Gunter, J.Huignard, Photorefractive Materials and Their Applications, Part 2 and 3, Springer Science+Business Media, New York (2007).
3. V.T.Potapov, T.V.Potapov, A.V.Kuchtaetal, *Photon-express*, **6**, 166 (2005).
4. T.V.Panchenko, N.A.Truseyeva, *Ferroelectrics*, **115**, 73 (1991).
5. I.Foldvard, I.E.Haliburrton., G.I.Edwards, *Solid State Comm.*, **77**, 181 (1991).
6. T.V.Panchenko, Z.Z.Yanchuk, *Phys. Solid State*, **38**, 1598 (1996).
7. V.V.Shepelevich, A.V.Makarevich, S.M.Shandarov, *Probl. Phys., Mat. Techn.*, **3**, 42 (2014).
8. A.A.Izvanov, A.E.Mandel, N.D.Chatkov et al., *Avtometriya*, **2**, 79 (1986).
9. D.A.Fish, A.R.Powel, T.J.Hall et al., *Opt. Comm.*, **98**, 349 (1993).
10. V.V.Shepelevich, *Journ. Techn. Phys.*, **56**, 618 (1986).
11. S.M.Shandarov, S.S.Chmakov, P.V.Zuevetal, *J. Opt. Technol.*, **80**, 409 (2013).
12. A.M.Plesovskikh, S.M.Shandarov, E.Yu.Ageev, *Phys. Solid State*, **43**, 251 (2001).
13. T.V.Panchenko, G.V.Snezhnoy, *Phys. Solid State*, **35**, 1598 (1993).
14. T.V.Panchenko, Yu.N.Potapovith., L.M.Karpova, *Ferroelectrics*, **122**, 1 (1998).
15. M.A.Bryushinin, *Techn. Phys.*, **49**, 1016 (2004).
16. Yu.Gorokhovatsky, H.Bordovsky, Termally Activational Current Spectroscopy of High-resistance Semiconductors and Dielectrics, Nauka, Moscow (1991) [in Russian].
17. C.Filipic, A.Klos, M.Gajc et al., *J. Adv. Dielectr.* **5**, 1550023 (2015).
18. V.K.Malinovskiy, O.A.Gudaev, V.A.Gusev et al., Photoinduzirovanie Yavleniya v Sillenitakh, Nauka, Novosibirsk (1990) [in Russian].
19. Sh.Lardhi, D.Nourekine, M.Harb et al., *J.. Chem. Phys.*, **144**, 134702-1 (2016).
20. A.F.Lima, S.A.Farias, M.V.Lalic, *J. Appl. Phys.*, **110**, 083705 (2011).
21. O.G.Vendik, A.I.Deduk, R.V.Dmitryev et al., *Fiz. Tverdogo Tela*, **26**, 684 (1984).
22. A.T.Shuvaev, V.G.Vlasenko, D.S.Drannikov et al., *Inorg.Mater.*, **41**, 1085 (2005).